

<b>Title of Grant / Cooperative Agreement:</b>	
<b>Type of Report:</b>	
<b>Name of Principal Investigator:</b>	
<b>Period Covered by Report:</b>	
<b>Name and Address of recipient's institution:</b>	
<b>NASA Grant / Cooperative Agreement Number:</b>	

**Reference 14 CFR § 1260.28 Patent Rights** (*abbreviated below*)

The Recipient shall include a list of any Subject Inventions required to be disclosed during the preceding year in the performance report, technical report, or renewal proposal. A complete list (or a negative statement) for the entire award period shall be included in the summary of research.

Subject inventions include any new process, machine, manufacture, or composition of matter, including software, and improvements to, or new applications of, existing processes, machines, manufactures, and compositions of matter, including software.

Have any Subject Inventions / New Technology Items resulted from work performed under this Grant / Cooperative Agreement?	No	Yes
If yes a complete listing should be provided here: Details can be provided in the body of the Summary of Research report.		

**Reference 14 CFR § 1260.27 Equipment and Other Property** (*abbreviated below*)

A Final Inventory Report of Federally Owned Property, including equipment where title was taken by the Government, will be submitted by the Recipient no later than 60 days after the expiration date of the grant. Negative responses for Final Inventory Reports are required.

Is there any Federally Owned Property, either Government Furnished or Grantee Acquired, in the custody of the Recipient?	No	Yes
If yes please attach a complete listing including information as set forth at § 1260.134(f)(1).		

***Attach the Summary of Research text behind this cover sheet.***

**Reference 14 CFR § 1260.22 Technical publications and reports (December 2003)**

Reports shall be in the English language, informal in nature, and ordinarily not exceed three pages (not counting bibliographies, abstracts, and lists of other media).

A Summary of Research (or Educational Activity Report in the case of Education Grants) is due within 90 days after the expiration date of the grant, regardless of whether or not support is continued under another grant. This report shall be a comprehensive summary of significant accomplishments during the duration of the grant.

# Investigation of Ice Particle Characteristics Through Comparison of APS and MODIS Measurements

## FINAL REPORT

Contract number: NNX11AR06G  
Activities: June 2011 - August 2015

Bryan A. Baum (PI), Space Science and Engineering Center  
University of Wisconsin-Madison, Madison, WI 53705  
[bryan.baum@ssec.wisc.edu](mailto:bryan.baum@ssec.wisc.edu)

Dr. Ping Yang (Co-I), Department of Atmospheric Sciences, Texas A&M University,  
College Station, TX 77843. Email: [pyang@tamu.edu](mailto:pyang@tamu.edu)

Dr. Steve Platnick (Co-I), NASA Goddard Space Flight Center, Greenbelt, MD  
Email: [steven.e.platnick@nasa.gov](mailto:steven.e.platnick@nasa.gov)

Dr. Jerome Riedi (Collaborator), Laboratoire d'Optique Atmospherique, Universite de Lille 1,  
Sciences et Technologies, Email: [jerome.riedi@univ-lille1.fr](mailto:jerome.riedi@univ-lille1.fr)

Dr. Zhibo Zhang, Physics Department, University of Maryland, Baltimore County. Email:  
[zhibo.zhang@umbc.edu](mailto:zhibo.zhang@umbc.edu) (working with Steve Platnick)

## Introduction

This report summarizes results for the period June 2012 – August 2015. This project was originally intended to be an observational study of the ice cloud microphysics and scattering properties using the multidirectional polarization measurements from the Aerosol Polarimeter Sensor (APS) on the NASA Glory platform. Due to the mishap of Glory's launch, the proposed work was no longer possible. The work split into two parts. Drs. Yang and Baum continued to develop ice cloud scattering properties for a set of ice habits that included the full phase matrix (necessary for analysis of polarimetric data), and then build bulk cloud models for use by the science community. The GSFC/UMBC team (Drs. Platnick and Zhang) shifted their research direction to theoretical studies using synthetic data and legacy observations from POLDER to better understand the fundamental principles and physics and explore new possibilities for remote sensing cloud properties from multidirectional polarization measurements.

As it turns out, both teams covered a significant amount of territory, with a number of research papers resulting from this work as demonstrated below. Based on work performed under this grant and under a previous grant (NNX11AF40G), ice models are available on the PI's web pages that are built consistently from the ultraviolet (UV) to the far-infrared (Far-IR). These models are being used in a variety of applications, including various remote sensing efforts, advanced radiative transfer models, and hyperspectral wavelength to broadband applications. While this work has been well received in the community, there is still much that we can offer. We hope that there will be future opportunities for funding in this area.

## Journal articles that acknowledge this grant

Yang, P., L. Bi, B. A. Baum, K.-N. Liou, G. Kattawar, and M. Mishchenko, 2013: Spectrally consistent scattering, absorption, and polarization properties of atmospheric ice crystals at wavelengths from 0.2  $\mu\text{m}$  to 100  $\mu\text{m}$ . *J. Atmos. Sci.*, **70**, 330-347.

Yi, B., X. Huang, P. Yang, B. A. Baum, and G. W. Kattawar: Considering polarization in MODIS-based cloud property retrievals by using a vector radiative transfer code. *J. Quant. Spectrosc. Radiat. Transfer*, **146**, 540-548, doi:10.1016/j.jqsrt.2014.05.020.

Cole, B. H., Yang, P., Baum, B. A., Riedi, J., and C.-Labonnote, L., 2014: Ice particle habit and surface roughness derived from PARASOL polarization measurements, *Atmos. Chem. Phys.*, **14**, 3739-3750, doi:10.5194/acp-14-3739-2014.

Baum, B. A., P. Yang, A. J. Heymsfield, A. Bansemer, A. Merrelli, C. Schmitt, and C. Wang: Ice cloud bulk single-scattering property models with the full phase matrix at wavelengths from 0.2 to 100  $\mu\text{m}$ . *J. Quant. Spectrosc. Radiat. Transfer*, **146**, 123-139, doi:10.1016/j.jqsrt.2014.02.029.

Hioki, S., P. Yang, B. A. Baum, S. E. Platnick, K. G. Meyer, M. D. King, and J. Riedi, 2015: Inference of the ice cloud particle roughness parameter in polarimetric data. On verge of submittal to *Atmospheric Chemistry and Physics*.

Miller, D. J., Z. Zhang, A. S. Ackerman, S. Platnick, and B. A. Baum, 2015: The impact of cloud vertical structure on cloud liquid water path retrieval based on the bi-spectral solar reflection method: A theoretical study based on large-eddy simulations. In preparation for submittal to *J. Quant. Spectrosc. Radiat. Transfer*.

## Progress made during the course of this grant

Both collectively and individually, this team has made some substantial progress over the past year, including the following tasks:

1. Drs. Bryan Baum and Ping developed and documented ice cloud bulk scattering models that contain the full phase matrix, making the models useful for working with polarized measurements. These models leverage the availability of a state-of-the-science database of the optical properties of various ice crystals (Yang, Bi and Baum and co-authors, 2013). This effort includes merging the ice crystal single-scattering properties and habit/size distributions and validating the resultant bulk optical and polarization properties.
2. Dr. Ping Yang's group has been conducting a global-scale survey of the degree of ice crystal surface roughness using POLDER measurements and modeling capabilities (Cole et al. 2014; Hioki et al. 2015). The development of the ice particle scattering property library was completed and documented in Yang et al. (2013). The library is unique in that it provides the full phase matrix for every ice habit at wavelengths from 0.2 to 100  $\mu\text{m}$ , and also includes 3 degrees of roughness from smooth to severely roughened surfaces.

3. Dr. Baum built and populated new set of web pages to provide background information, software, and models as they become available ([http://www.ssec.wisc.edu/ice\\_models](http://www.ssec.wisc.edu/ice_models)). The web pages provide background and methodology information. Spectral models between 0.2 and 100  $\mu\text{m}$  that contain the full phase matrix and imager models (currently for about three dozen polar-orbiting and geostationary sensors) are currently available via web page access. The paper that documents this full wavelength range of spectral models was published last fall (Baum et al. 2014).
4. Drs. Zhang and Platnick developed a numerical simulator based on synthetic cloud fields from large-eddy simulations (LES) and polarized radiative transfer models to simulate the multidirectional, multispectral polarization measurements from satellite-based polarimeter. This simulator is highly useful not only for fundamental theoretical studies, but also for evaluating instrument design concepts such as trade-off between spatial and angular resolution, spectral coverage, etc. to support future NASA missions (e.g., PACE).
5. Dr. Zhang and his PhD student, Daniel Miller, investigated how the polarimeter-based cloud microphysical property retrieval algorithm is influenced by cloud vertical structure and horizontal heterogeneity, and how to use the polarimetric observations to improve the cloud optical thickness and cloud droplet effective radius retrievals based on the MODIS-like bi-spectral method. The paper stemming from this research is in preparation and will soon be submitted: Miller et al. (2015), with full reference provided earlier in this report.

## Research Highlights

### 1. Comparison of PARASOL measurements to simulations based on a general habit mixture (GHM) (work by Baum and Yang)

As part of this grant, we completed 3 sets of ice cloud bulk scattering property models that span wavelengths from 0.2 to 100  $\mu\text{m}$ . One set is based on severely roughened solid columns only (similar to what the CERES team has been using), a second set is based on a severely roughened aggregate of solid columns (similar to what is being used for MODIS Collection 6 products), and a third set is based on a general habit mixture (GHM) of severely roughened particles rather than a single habit. Passive imagers, such as MODIS and VIIRS, only measure intensity, i.e., the  $P_{11}$  component of the phase matrix. However, there is a wealth of information that can be gained from other components, some of which is available from a polarimeter like PARASOL. With our bulk scattering models, we demonstrated that use of a general habit mixture (GHM), assuming severe particle roughening, for a range of  $D_{eff}$  values results in consistent comparisons with measured reflectivities for a single day of global PARASOL data over ocean (Cole et al. 2013). With a habit mixture, we were able to achieve quite a close comparison over a large range of scattering angles, similar to what is shown in Figure 1. A question that was not addressed is whether this same model will result in consistent comparisons with PARASOL over time. Figure 1 shows similar comparisons for one day in each of four different seasons, based on the GHM for  $D_{eff}=60 \mu\text{m}$ . The simulations generally match well with PARASOL measurements over the range of scattering angles for each of these days.

We also note that the use of severely roughened particles has another benefit. One of the issues with MODIS Collection 5 optical thickness values for ice clouds was that they were higher than those from the CALIPSO lidar. The Collection 5 ice models assumed smooth ice particles. By

adopting roughened particles, the amount of scattering in the forward direction is decreased, thereby lowering the asymmetry parameter. The short story is that the use of severely roughened particles greatly decreases the differences between MODIS optical thickness values and those from CALIPSO, and also leads to smaller differences between MODIS and PARASOL. Our models are percolating through the community and are being cited in publications regularly. To summarize, use of our models lead to greater consistency between the different measurements provided in the NASA A-Train.

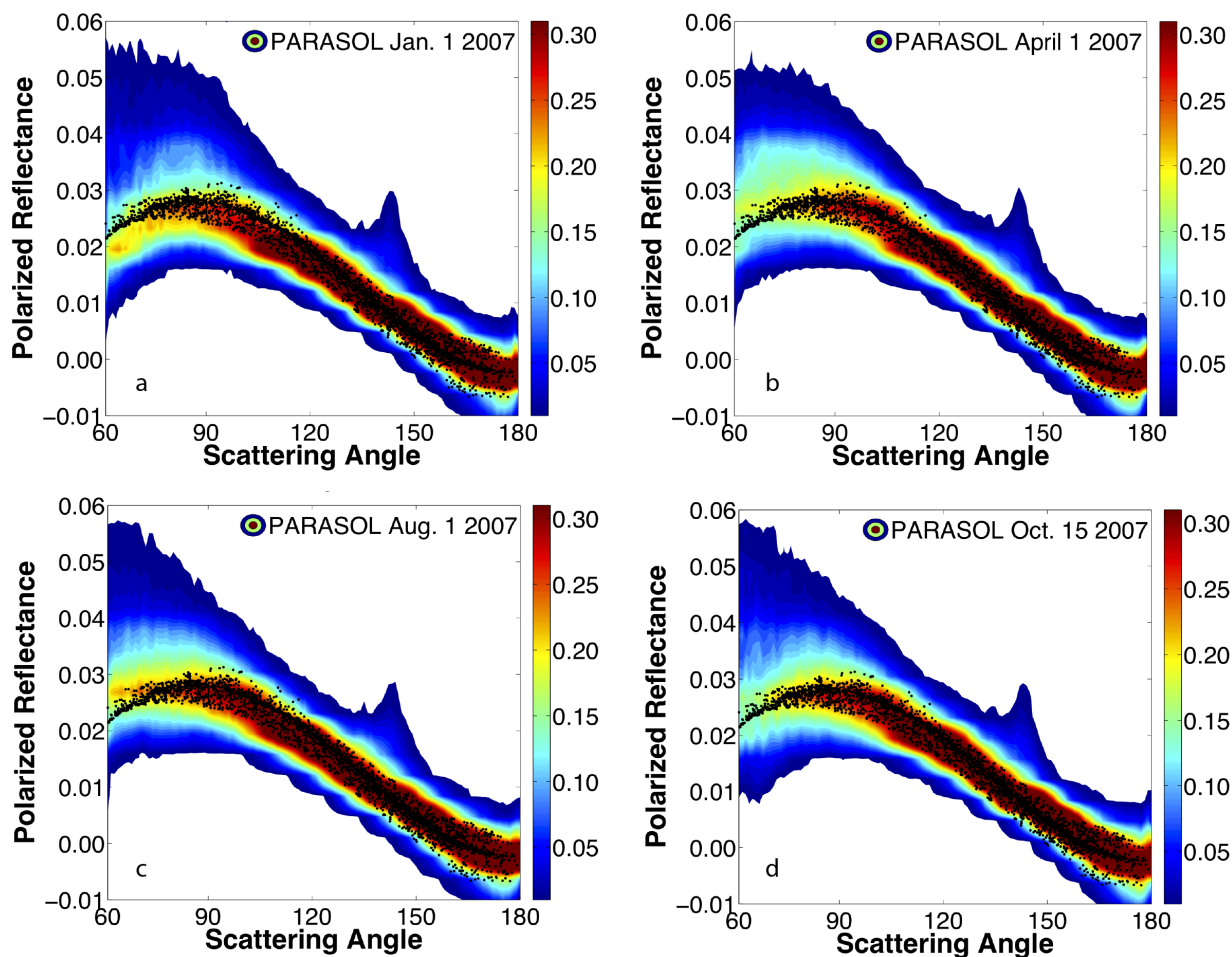


**Figure 1.** Comparison of PARASOL measurements of ice cloud polarized reflectivities over ocean (in the color contours) with simulations (black dots) based on ice model bulk scattering properties developed using a general habit mixture (GHM) assuming  $D_{eff}=60 \mu\text{m}$  for one day in four seasons: (a) 1 January, 2007, (b) 1 April, 2007, (c) 1 August, 2007, and 15 October, 2007. Note that the black dots mimic the PARASOL polarized reflectivities consistently for all four days.

We note that this use of polarimetric data opened up new doors for developing the next generation of scattering properties for MODIS retrievals. In a study on the verge of submission (Hioki et al. 2015), a new way of inferring the ice particle roughness is explored that is based on empirical orthogonal function (EOF) analysis and proper treatment of polarization due to atmospheric scattering above the cloud layer. In this study, a global one-month PARASOL data analysis supports the use of a severely roughened ice habit to simulate the polarized reflectivity

from ice clouds over the oceans. The density distribution of the roughness parameter inferred from the global one-month data sample demonstrates the significant variability of ice cloud scattering properties. By definition of our EOF scores, the inverted EOF scores translate into  $-P_{12}$  on a pixel-by-pixel basis. The reconstructed  $-P_{12}$  reflects a variation due to observation error and natural variability. To accurately interpret the result, we reconstructed  $-P_{12}$  from extratropical data with a precise EOF 2 score ( $SD(EOF\ 2) < 0.01$ ). The area shaded with gray in Fig. 2 shows the interquartile range of the reconstructed  $-P_{12}$  which indicates that 50% of our extratropical observations fall within the shade at a given scattering angle. The blue line is  $-P_{12}$  for the particle shape used in MODIS Collection 6, and the green line is that for the shape in MODIS Collection 5. Both particle models assume a gamma distribution with effective particle size of  $60\ \mu\text{m}$  and effective variance of 0.1. The blue line (Collection 6) is closer to our reconstruction, while the green line (Collection 5) significantly deviates from our reconstruction. This result indicates that the particle habit adopted for MODIS Collection 6 is more consistent with polarimetric observations than the habit mixture used for MODIS Collection 5, for which only one of the habits included a limited degree of roughness. We also find that better consistency is obtained with a mixture of two habits: 70% column aggregate particles with roughness parameter of  $\sigma^2=0.8$  and 30% severely roughened hollow bullet rosette particles ( $\sigma^2=0.8$ ) included in the scattering property library by Yang et al. (2013), as indicated by the thick magenta line in Fig. 2.

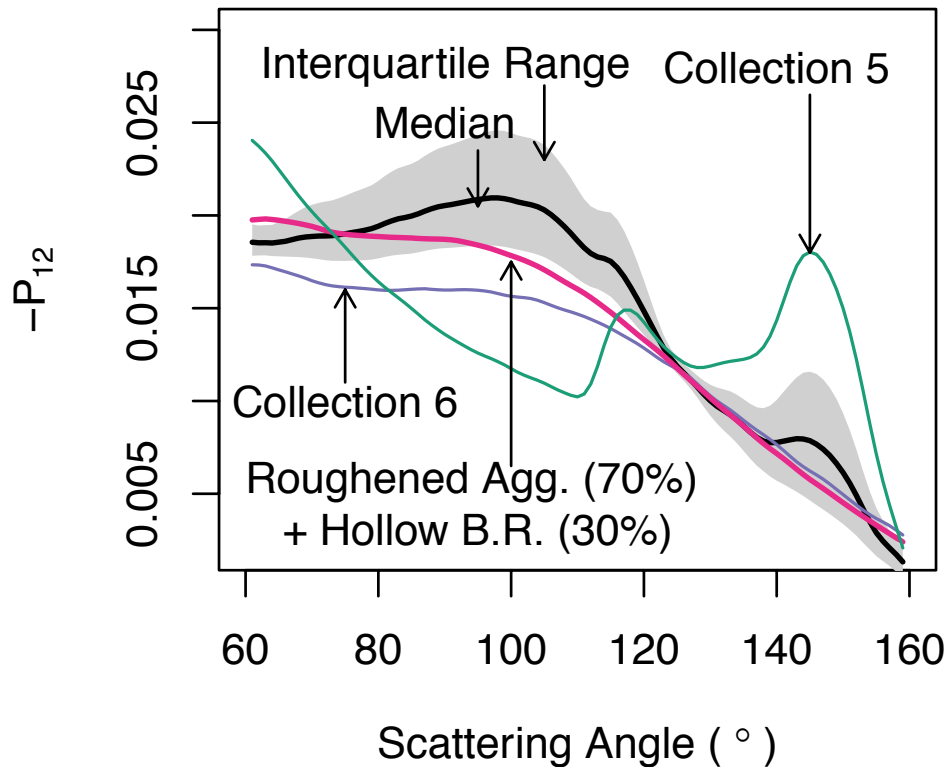


**Figure 2:** Comparison of the inferred  $-P_{12}$  values to those calculated from the MODIS Collection 5 and 6 models. The  $-P_{12}$  of MODIS Collection 6 (blue line) is more consistent with the reconstructed  $-P_{12}$  (black thick line) than the  $-P_{12}$  of MODIS Collection 5 (green line). However, better consistency is obtained with a two-habit model (thick magenta line), by increasing the roughness to  $\sigma^2=0.8$  and adding 30% of hollow bullet rosette particles.

## 2. Development of a numerical simulator for simulating satellite-based polarimeter measurements using LES and radiative transfer models (Zhang, Platnick, and colleagues)

We developed a numerical simulator based on synthetic cloud fields from a LES model with bin microphysics scheme and polarized radiative transfer models for simulating satellite based multidirectional, multispectral polarimetric measurements. The LES model developed by Andrew Ackerman (NASA GISS) is able to simulate the variations of cloud physical (i.e., LWC) and microphysical (i.e., droplet size distributions) properties at very high-resolution ( $\sim 50$  m) that are much smaller than the resolution of most current satellite sensors ( $\sim$ km). This provides us an opportunity to study how sub-pixel cloud variability influences cloud property retrievals from satellite sensors, including polarimeter. The simulator is backboneed by two radiative transfer models. The first one is a polarized 1-D radiative model based on the Doubling-Adding technique (de Haan et al., 1987) and the other is a polarized 3-D radiative transfer model based on Monte-Carlo technique developed by Cornet et al. (2010). The capability of simulating both 1-D and 3-D radiative transfer enables us to study the impact of 3-D effects on cloud property retrievals.

An example case from this simulator is shown in Figure 3. The LES cloud field is simulated based on the meteorological conditions observed during the DYCOMS-II field campaign. Here, we are simulating a satellite instrument that scans the cloud field from left to right at different viewing angles. Because the solar angles are fixed, the variation of viewing angles relates to a range of scattering angles (Fig. 3c). Figure 3a shows the true color image of the LES cloud field based on the simulated total reflectance in 0.49  $\mu\text{m}$  (blue), 0.55  $\mu\text{m}$  (green) and 0.86  $\mu\text{m}$  (red) band. Note the slight color dispersion around the center of the image, which corresponds to the cloudbow around the  $140^\circ$  scattering angle; Figure 3b shows the false color image of the cloud field based on simulated *polarized* reflectance in 0.49  $\mu\text{m}$  (blue), 0.55  $\mu\text{m}$  (green) and 0.86  $\mu\text{m}$  (red) band; The bright band in the figure corresponds to the strong polarized reflectance in the primary cloudbow scattering region. The secondary blue band to the right of the primary cloudbow is the supernumerary cloudbow centered around the  $150^\circ$  scattering angle. The color dispersion in the supernumerary cloudbow is more evident, which can be used to infer the effective particle size of the cloud (Breon and Doutriaux-Boucher, 2005).

This example clearly demonstrates the capability of the simulator. It is highly useful not only for fundamental theoretical studies, but also for evaluating instrument design concepts such as trade-off between spatial and angular resolution, spectral coverage, etc. to support future NASA missions (e.g., PACE).

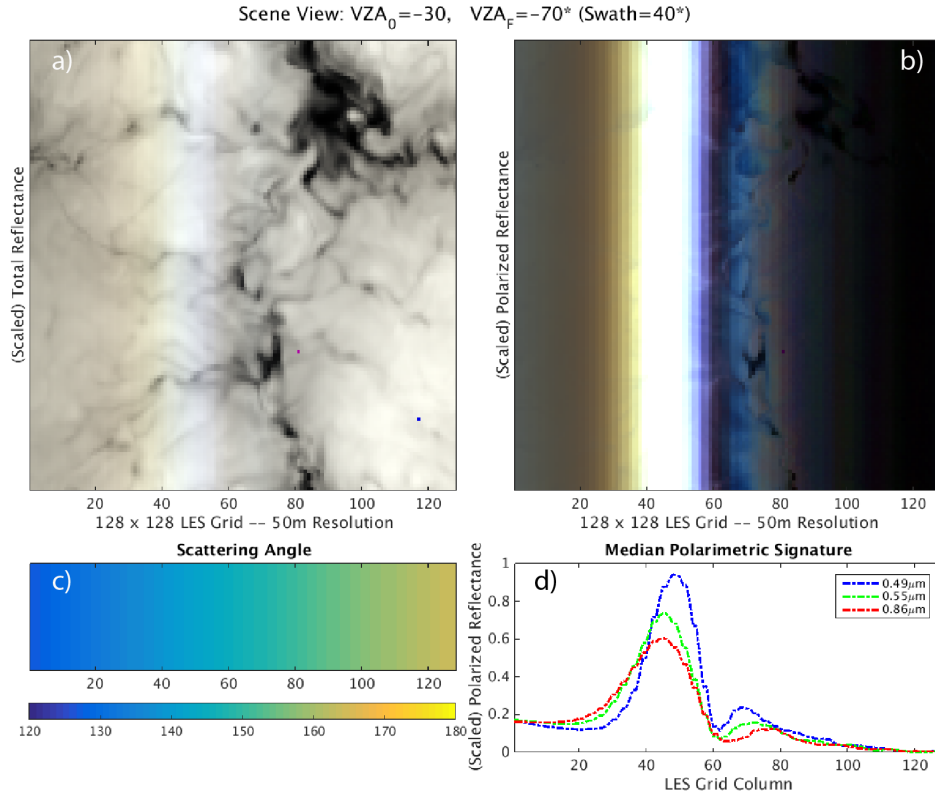


**Figure 3.** A synthetic RGB image of a LES cloud field based on simulated total reflectance in 0.49  $\mu\text{m}$  (blue), 0.55  $\mu\text{m}$  (green) and 0.86  $\mu\text{m}$  (red) band; note the color dispersion in the cloudbow region; b) a synthetic false color image of the cloud field based on simulated polarized reflectance in 0.49  $\mu\text{m}$  (blue), 0.55  $\mu\text{m}$  (green) and 0.86  $\mu\text{m}$  (red) band; the bright band in the figure corresponds to the strong polarized reflectance in the primary cloudbow scattering region. c) the viewing and scattering angles d) the polarized reflectances as a function of scattering angle.

### 3. Using polarimetric observations to improve the cloud droplet size retrievals based on MODIS-like bi-spectral method (Zhang and colleagues)

The bi-spectral solar reflective method first introduced by Nakajima and King (1990) is a widely used method for inferring cloud optical thickness ( $\tau$ ) and cloud droplet effective radius ( $r_e$ ) from satellite observations. This method utilizes a pair of cloud reflection observations, one in the visible/near-infrared (VIS/NIR), and the other in the shortwave-infrared (SWIR) spectral region, to simultaneously retrieve  $\tau$  and  $r_e$ . The bi-spectral method requires several important assumptions and simplification, one of which is that the effective variance ( $v_e$ ) of cloud top droplet size distribution is a constant often assumed to be around 0.1 (e.g., MODIS operational product). Hereafter, we refer this assumption as constant  $v_e$  assumption.

With use of the satellite observation simulator described above, we recently investigated the impact of constant  $v_e$  assumption on bi-spectral  $\tau$  and  $r_e$ , and how to use polarimetric measurements to improve the retrievals (manuscript in preparation: Miller et al. 2015). The main findings from this study are summarized in Figure 4 and Figure 5. The cloud field used in this



study is the DYCOMS-II case in Figure 3. The  $r_e$  retrieval based on the bi-spectral method using the combination of  $0.86\ \mu\text{m}$  and  $3.7\ \mu\text{m}$  cloud reflectances are shown in Figure 4a. Note that in this retrieval the  $v_e$  is assume to be a constant 0.1. Figure 4b shows the  $r_e$  retrieval from the simulated multi-angular polarimetric observations. A comparison of the retrievals from the two methods is shown in Figure 4c. We note that the results from the bi-spectral method tend to be larger than from the polarimetric method and the differences seem to be linked to the value of  $v_e$  at cloud top. The  $r_e$  retrievals are significantly larger (up to  $3\ \mu\text{m}$ ) in regions where  $v_e < 0.1$  than with the polarimetric retrievals.

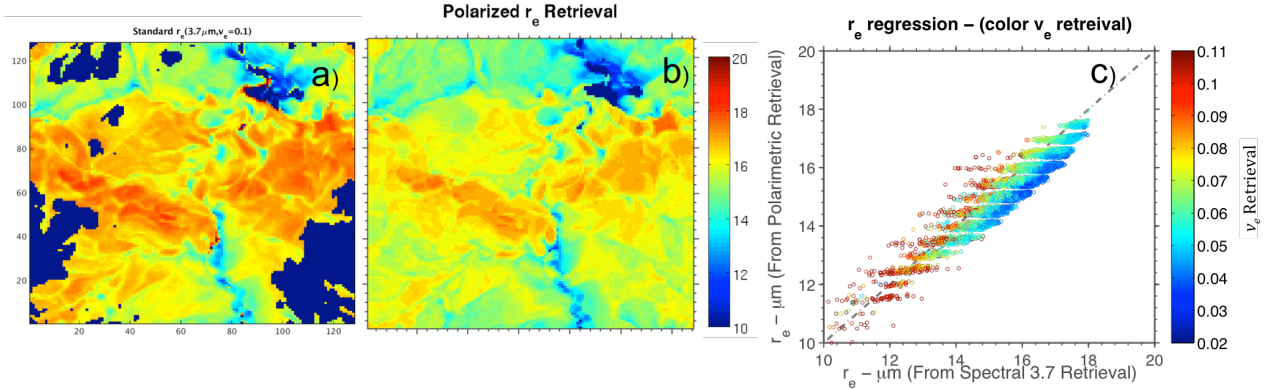


**Figure 4.** a) cloud droplet effective radius retrieval based on the bi-spectral method using the combination of  $0.86\ \mu\text{m}$  and  $3.7\ \mu\text{m}$  cloud reflectance observation. b) cloud droplet effective radius retrieval from multi-angular polarimetric observations; c) scatter plot comparison of the retrievals from the two method. The color in the figure corresponds to the effective variance retrievals from polarimetric method.

Inspired by this result, we developed a simple research-level method that uses the  $v_e$  retrievals from the polarimetric observation to help the  $r_e$  retrieval based on the bi-spectral method. In this method, we add another dimension to the look-up-table used in the bi-spectral method, so that it is a function of not only  $\tau$  and  $r_e$ , but also  $v_e$ . In the retrieval process, we first derive the  $v_e$  from the polarimetric measurement and then use it to select the proper LUT for  $\tau$  and  $r_e$  retrievals. As shown in Figure 5, the  $r_e$  retrieval based on the new method is closer to the  $r_e$  retrieval from the polarimetric method. We are now investigating whether the  $r_e$  retrieval from the new method helps us to better understand the original cloud field, for example whether the new retrievals help to better quantify the radiative properties, such as angular distribution and spectral signature, of the cloud with significant vertical structure.

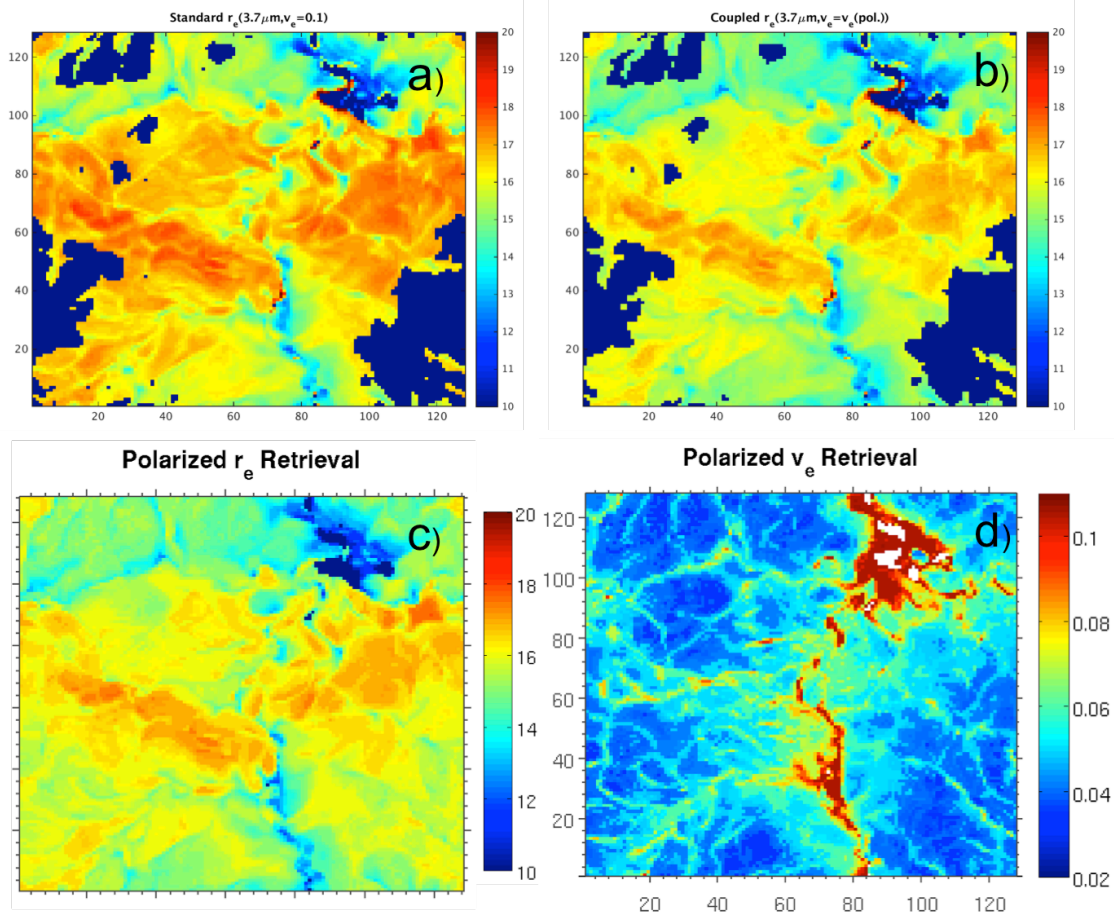


**Figure 5.** a) cloud  $r_e$  retrieval based on the bi-spectral method under the constant  $v_e=0.1$  assumption. b) bi-spectral  $r_e$  retrieval based the new method; c)  $r_e$  and d)  $v_e$  retrievals from the polarimetric retrieval.

## Other References

- Bréon, F. M., and M. Doutriaux-Boucher (2005), A comparison of cloud droplet radii measured from space, *Geoscience and Remote Sensing, IEEE Transactions on*, 43(8), 1796–1805, doi:10.1109/TGRS.2005.852838.
- Cole, B., P. Yang, B.A. Baum, J. Riedi, C.-L. Labonnote, F. Thieuleux, and S. Platnick, 2013: Comparison of PARASOL observations with polarized reflectances simulated using different ice habit mixtures. *J. Appl. Meteor. Clim.* 52: 186-196.
- Cornet, C., L. C-Labonnote, and F. Szczap (2010), Three-dimensional polarized Monte Carlo atmospheric radiative transfer model (3DMCPOL): 3D effects on polarized visible reflectances of a cirrus cloud, *Journal of Quantitative Spectroscopy and Radiative Transfer VL -*, 111(1), 174–186, doi:10.1016/j.jqsrt.2009.06.013.
- de Haan, J., P. Bosma, and J. Hovenier (1987), The adding method for multiple scattering calculations of polarized light, *Astron. Astrophys.*, 183, 371–391.
- Nakajima, T., and M. D. King (1990), Determination of the Optical Thickness and Effective Particle Radius of Clouds from Reflected Solar Radiation Measurements. Part I: Theory, *Journal of Atmospheric Sciences*, 47(15), 1878–1893, doi:10.1175/1520-0469(1990)047<1878:DOTOTA>2.0.CO;2.